

Microbial community structure of hydrothermal deposits from geochemically different vent fields along the Mid-Atlantic Ridge

Gilberto E. Flores,¹ James H. Campbell,²
Julie D. Kirshtein,³ Jennifer Meneghin,¹
Mircea Podar,² Joshua I. Steinberg,⁴
Jeffrey S. Seewald,⁵ Margaret Kingston Tivey,⁵
Mary A. Voytek,^{3,6} Zamin K. Yang² and
Anna-Louise Reysenbach^{1*}

¹Department of Biology, Portland State University,
Portland, OR 97201, USA.

²Biosciences Division, Oak Ridge National Laboratory,
Oak Ridge, TN 37830, USA.

³United States Geological Survey, Reston, VA 20192,
USA.

⁴Oregon Episcopal School, Portland, OR 97223, USA.

⁵Marine Chemistry and Geochemistry Department,
WHOI, Woods Hole, MA 02543, USA.

⁶National Aeronautics and Space Administration,
Washington, DC 20546, USA.

Summary

To evaluate the effects of local fluid geochemistry on microbial communities associated with active hydrothermal vent deposits, we examined the archaeal and bacterial communities of 12 samples collected from two very different vent fields: the basalt-hosted Lucky Strike (37°17'N, 32°16.3'W, depth 1600–1750 m) and the ultramafic-hosted Rainbow (36°13'N, 33°54.1'W, depth 2270–2330 m) vent fields along the Mid-Atlantic Ridge (MAR). Using multiplexed barcoded pyrosequencing of the variable region 4 (V4) of the 16S rRNA genes, we show statistically significant differences between the archaeal and bacterial communities associated with the different vent fields. Quantitative polymerase chain reaction (qPCR) assays of the functional gene diagnostic for methanogenesis (*mcrA*), as well as geochemical modelling to predict pore fluid chemistries within the deposits, support the pyrosequencing observations. Collectively, these results show that the less reduced, hydrogen-poor fluids at Lucky Strike limit colonization by strict anaerobes

such as methanogens, and allow for hyperthermophilic microaerophiles, like *Aeropyrum*. In contrast, the hydrogen-rich reducing vent fluids at the ultramafic-influenced Rainbow vent field support the prevalence of methanogens and other hydrogen-oxidizing thermophiles at this site. These results demonstrate that biogeographical patterns of hydrothermal vent microorganisms are shaped in part by large scale geological and geochemical processes.

Introduction

Deep-sea hydrothermal environments support highly productive biological communities comparable in total biomass production to the most prolific marine ecosystems (Sarrazin and Juniper, 1999). As the high-temperature hydrothermal fluid mixes with cold oxygenated seawater, minerals precipitate to form vent mineral deposits (Tivey, 2007). These porous deposits are quickly colonized by a diversity of *Archaea* and *Bacteria* that harness the abundant geochemical energy available in the hydrothermal fluids (Page *et al.*, 2008). One of the major processes controlling the chemical composition of hydrothermal fluids is the interaction of subsurface circulating seawater with surrounding igneous rocks at elevated temperatures and pressures (Von Damm, 1995). The majority of magmatically heated vent systems thus far studied are hosted by basaltic rocks and give rise to fluids rich in hydrogen-sulfide (Von Damm, 1995). However, along slow- and ultra-slow-spreading ridges like the Mid-Atlantic Ridge (MAR), some hydrothermal systems include reactions with ultramafic rocks (peridotite), which have significant impacts on fluid chemistry. For example, due to serpentinization reactions, hydrothermal fluids can have elevated concentrations of hydrogen (H₂), iron (Fe) and methane (CH₄), and lower levels of hydrogen-sulfide (H₂S) relative to basalt-hosted systems (Charlou *et al.*, 2002) (Table 1).

While numerous molecular- and cultivation-based studies have been conducted to document the diversity of microorganisms associated with hydrothermal vent deposits, relatively few studies have explored the possible abiotic controls on microbial biogeography in these systems. Theoretically, the type and magnitude of energy

Received 3 November, 2010; accepted 29 January, 2011. *For correspondence. E-mail reysenbacha@pdx.edu; Tel. (+1) 503 725 3864; Fax (+1) 503 725 3888.

Table 1. Range of physicochemical characteristics of end-member hydrothermal fluids from different vent fields along the Mid-Atlantic Ridge.

	Basalt-hosted			Ultramafic-hosted			Seawater
	13°N (EPR)	TAG	Lucky Strike	Rainbow	Logatchev	Lost City	
Temperature (°C)	317–380	290–321	163–324 (172–324)	191–370 (365)	347–353	40–75	4
pH (25°C)	ND	3.1	3.6–3.9 (3.5–3.7)	3.0–3.4 (2.8)	3.3–3.9	9.0–9.8	8.1
H ₂ (mM)	0.14	0.15–0.37	0.025–0.071 (0.003–0.73)	12.3–16.9 (16)	12–19	0.25–0.43	0.0004
H ₂ S (mM)	2.9–8.2	6.7	2.4–3.4 (2.0–3.0)	1.8–3.3 (1.2)	0.5–2.5	0.064	0
CH ₄ (mM)	0.051	0.124–0.147	0.77–1.1 (0.30–0.85)	1.9–2.3 (2.5)	2.1–3.5	0.13–0.28	0.0003
CO ₂ (mM)	11.8–18.4	2.9–3.4	35–133 (15.1–39.9)	21–25 (16)	10.1	ND	2.3
Fe (µM)	1450–10 800	1640	ND (31–863)	8100–24 100 ^a (24 050)	2410–2500	ND	0.0045
Reference	Von Damm (1995)	Charlou <i>et al.</i> (2002)	This work	This work	Charlou <i>et al.</i> (2002); Schmidt <i>et al.</i> (2007)	Kelley <i>et al.</i> (2001)	Charlou <i>et al.</i> (2002); Schmidt <i>et al.</i> (2007)

a. Iron values reported are from Seyfried and colleagues (2011) and were collected during the same research cruise as the deposits used in this study.

Values reported for Lucky Strike and Rainbow were determined as part of this study. Values in parentheses for Lucky Strike and Rainbow have been added for comparison and are from Charlou and colleagues (2000) and Charlou and colleagues (2002), respectively. Fluids from 13°N along the East Pacific Rise and seawater are added for comparison.

TAG, Trans-Atlantic Geotraverse; EPR, East Pacific Rise; ND, not determined.

sources available in the hydrothermal fluids have been predicted to play a major role in determining the distribution patterns of deep-sea vent microorganisms (Shock *et al.*, 1995; Shock and Holland, 2004; Tivey, 2004; Takai *et al.*, 2006a; McCollom, 2007; Takai and Nakamura, 2010). Of the studies that have attempted to link hydrothermal fluid chemistry with microbial community composition, most have focused on single vent fields and have been hampered by inadequate sample number and/or sequencing depth (Takai *et al.*, 2004; 2008; Nakagawa *et al.*, 2005a; Sogin *et al.*, 2006; Huber *et al.*, 2007; Perner *et al.*, 2007; Nunoura and Takai, 2009; Opatkiewicz *et al.*, 2009; Takai and Nakamura, 2010). Recently, Huber and colleagues (2010) overcame these limitations by employing next generation sequencing techniques to characterize the bacterial communities of diffuse fluid samples at five seamounts along the Mariana Arc. While the study revealed non-random distribution patterns of the dominant *Epsilonproteobacteria*, correlations between hydrothermal fluid chemistry and the observed patterns were not apparent. Several factors, including the inability to detect fine-scale patterns with short 16S ribosomal RNA (rRNA) gene fragments from the hypervariable region 6 (V6), were suggested as possible reasons as to why community structure was not correlated with fluid chemistry. As such, the impact of hydrothermal fluid chemistry on microbial community composition and/or structure remains largely unknown.

As the potential for direct coupling of geochemistry and biology is greatest at the interface where the hydrothermal fluids mix with seawater to produce mineral deposits, we

hypothesized that the microbial communities associated with active vent deposits would be different in vent fields of contrasting chemistry. To address this question, we characterized the archaeal and bacterial communities of 12 deposits from two magmatically heated hydrothermal systems: the ultramafic-hosted Rainbow (36°13'N, 33°54.1'W, depth 2270–2330 m) and the basalt-hosted Lucky Strike (37°17'N, 32°16.3'W, depth 1600–1750 m) vent fields along the MAR (Fig. S1, Table S1). Due to the relatively close proximity of the two vent fields (approximately 180 km apart), the likelihood that any observed differences are due to a distance–decay relationship is minimized, and therefore provide model sites for assessing the impact that geological processes controlling fluid chemistry have on microbial biogeography. Both vent fields have been fairly well characterized with respect to fluid chemistry (Langmuir *et al.*, 1997; Von Damm *et al.*, 1998; Charlou *et al.*, 2002; Douville *et al.*, 2002), geologic setting (Langmuir *et al.*, 1997; Charlou *et al.*, 2002; Douville *et al.*, 2002; Humphris *et al.*, 2002; Singh *et al.*, 2006), deposit mineralogy (Rouxel *et al.*, 2004a,b; Marques *et al.*, 2006) and macrobiological communities (Desbruyeres *et al.*, 2000; 2001).

The Rainbow vent field is located within ultramafic rocks on the western flank of a non-volcanic ridge at the intersection between the non-transform system faults and the ridge faults (Douville *et al.*, 2002). The vent field is tectonically controlled and is composed of at least 10 active chimneys that emit acidic, high-temperature fluids (370°C) with relatively consistent end-member compositions indicative of a single source for the entire field

(Charlou *et al.*, 2002). Hydrothermal fluids from Rainbow are influenced by serpentinization reactions and are characterized by high dissolved gas, particularly H₂, CH₄ and CO, and metal concentrations but relatively low H₂S concentrations (Table 1) (Charlou *et al.*, 2002; Douville *et al.*, 2002). Minerals present in these chimneys include pyrrhotite and isocubanite, indicative of relatively reducing environments (Rouxel *et al.*, 2004a).

The Lucky Strike vent field is located at the summit of the Lucky Strike seamount along the MAR near a young, solidified lava lake and is one of the largest vent fields along the MAR (Langmuir *et al.*, 1997; Humphris *et al.*, 2002). Hydrothermal activity here has been episodic but ongoing for hundreds to thousands of years (Humphris *et al.*, 2002). The fluids from Lucky Strike originate from reactions with relatively oxic, and previously altered basalt, and are somewhat unique for a basalt-hosted system with respect to the relatively high pH (25°C) and low Fe, manganese (Mn), lithium (Li) and zinc (Zn) concentrations (Von Damm *et al.*, 1998). Minerals present in chimneys and flanges include pyrite, marcasite, chalcopyrite and sphalerite, indicative of relatively more oxidizing conditions than at the Rainbow vent field (Langmuir *et al.*, 1997; Rouxel *et al.*, 2004b). There is also evidence that fluids from Lucky Strike may have two sources as fluids from the northern segment are systematically different than those from the south (Von Damm *et al.*, 1998). Unlike fluids from Rainbow, the predominant gas in Lucky Strike fluids is CO₂ with H₂ two to three orders of magnitude less in concentration (Table 1) (Von Damm *et al.*, 1998; Charlou *et al.*, 2002). Such dramatic differences in H₂ concentrations are likely to be a strong force in structuring hydrothermal vent microbial communities as has been previously predicted (Shock *et al.*, 1995; Shock and Holland, 2004; Takai *et al.*, 2006a; McCollom, 2007; Takai and Nakamura, 2010) since many chemosynthetic primary producers utilize H₂ as an energy source.

Results and discussion

Alpha- and beta-diversity

Because of the limitations of using the V6 region of the 16S rRNA gene in multiplexed barcoded pyrosequencing (Claesson *et al.*, 2009; Huber *et al.*, 2010; Schloss, 2010), we targeted the V4 region to characterize the archaeal and bacterial communities associated with hydrothermal deposits. Using this approach, we generated 45 195 and 91 607 high-quality archaeal (average 3766 sequences per sample, 247–249 nt length) and bacterial (average 7634 sequences per sample, 207–208 nt length) sequences, respectively (Table S1). Pyrosequencing amplicons were aligned and clustered using the Ribosomal Database Projects (RDP) pyrosequencing and the

SLP/PW-AL pipelines at operational taxonomic unit (OTU) definitions of 95% and 97% sequence similarity, respectively (Cole *et al.*, 2009; Huse *et al.*, 2010). Alpha-diversity assessments (OTU richness, Chao1 index and rarefaction analysis) revealed comparable results with both alignment/clustering approaches (Fig. S2, Table S2) providing us with confidence that overestimates of diversity were minimized. Overall, bacterial diversity was greater than archaeal diversity in all samples. Furthermore, several of the archaeal rarefaction curves are near-asymptotic, indicating that we have nearly completely sampled the archaeal V4 diversity of these samples (Fig. S2).

Differences in overall community composition between vent fields (beta-diversity) were assessed using both OTU-based metrics (Bray-Curtis, Sørensen) and the phylogeny-based metric, UniFrac (Lozupone *et al.*, 2006; Hamady *et al.*, 2010). UniFrac distances were calculated to account for abundances of individual taxa (weighted) or based solely on presence/absence (unweighted). Non-metric multidimensional scaling (MDS) plots built using all metrics revealed that the communities from the two vent fields were distinct (Fig. 1A and B, Fig. S3A–F). Statistically significant patterns, as determined by ANOSIM (Primer v6), were observed in seven of the eight analyses (Fig. 1A and B, Fig. S3A–F) with the sole exception being the bacterial weighted UniFrac distances. It is likely that the dominance of closely related *Epsilonproteobacteria* in the bacterial data mask the significant differences observed using the unweighted UniFrac distances, although the bacterial communities were significantly different in both weighted (Bray-Curtis) and unweighted (Sørensen) OTU-based analyses. Moreover, we found that the archaeal and bacterial community composition varied significantly less within vent fields than between vent fields and hence, community composition was more similar within than between vent fields (Fig. 1C, Fig. S3G–I). This suggests that the geochemical differences between the two vent fields are a stronger force in structuring microbial communities than any within vent field force. Together, these results clearly show that the microbial communities are different between the Rainbow and Lucky Strike vent fields.

Taxonomy

While beta-diversity metrics provide insights into overall community differences, assigning taxonomic identities to sequences allows for determining how these communities differ taxonomically and possibly functionally. To achieve this, we used the RDP classifier (Wang *et al.*, 2007) set at a bootstrap value of 50% (Claesson *et al.*, 2009) to classify representative sequences of each OTU defined using the RDP-95% clusters. Manual classifications using ARB

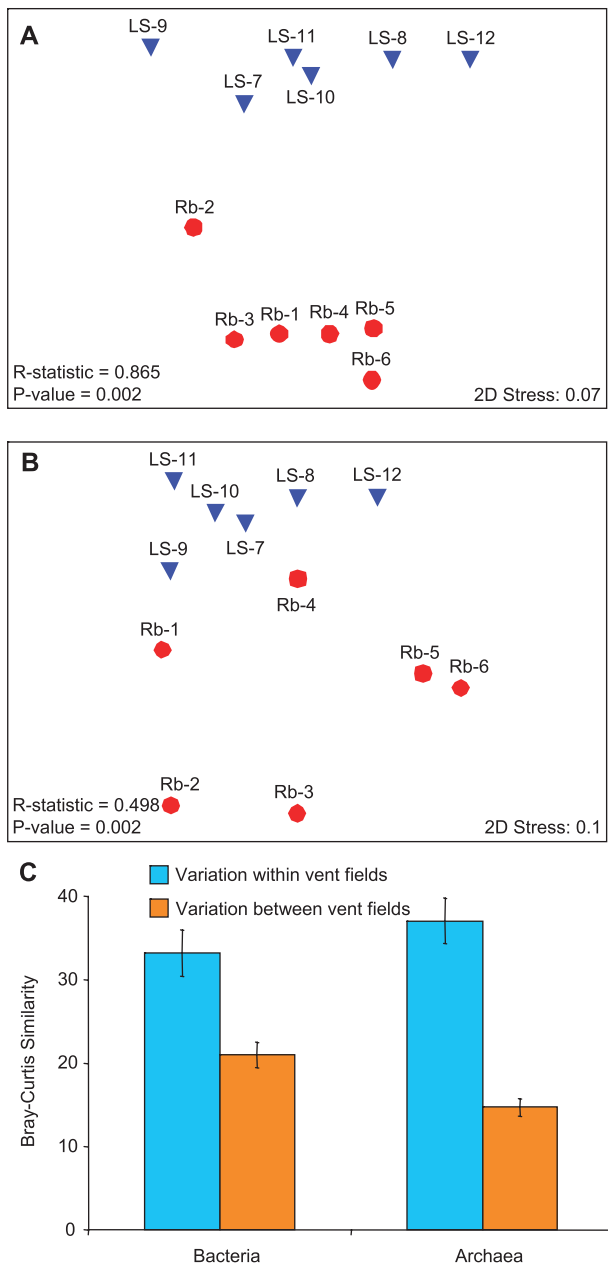


Fig. 1. 16S rRNA gene surveys reveal partitioning of the archaeal and bacterial communities between the ultramafic-hosted Rainbow (red) and basalt-hosted Lucky Strike (blue) vent fields along the Mid-Atlantic Ridge.

A and B. Communities clustered using MDS of the Bray-Curtis similarities for archaeal (A) and bacterial (B) communities. Each point represents an individual vent sample. Results of ANOSIM analysis showing that the observed patterns are significant are presented in the bottom left corner of each plot.

C. Average Bray-Curtis similarity within and between vent fields. Average distances were significantly different for both archaeal and bacterial communities as determined by one-tailed *t*-tests ($P < 0.001$). Error bars indicate the standard error of the mean (SEM).

(Ludwig *et al.*, 2004) and BLAST were also performed for many unclassified OTUs as known lineages (e.g. 'Aciduliprofundales') were not classified by the RDP classifier.

Archaea

Overall, the archaeal lineages observed at both vent fields were typical for this environment and likely represent the core archaeal microbiome. Archaeal families shared between all vent samples include the thermophilic *Desulfurococcaceae*, *Thermococcaceae* and *Thermofilaceae* (Fig. 2A). Other thermophilic lineages shared by most samples include the mixotrophic *Archaeoglobaceae*, the acidophilic fermentative 'Aciduliprofundales' (DHVE2) and the *Nanoarchaea* (Takai and Horikoshi, 1999; Boone *et al.*, 2001; Huber *et al.*, 2002; Reysenbach *et al.*, 2006; Reysenbach and Flores, 2008). Several novel lineages with no known isolates in culture were also observed. For example, three OTUs ('Unclassified *Euryarchaeota* A') were found in all but three samples. Sequences of these OTUs are related to clones found in other deep-sea vent environments (> 94% similarity) (Moussard *et al.*, 2006). Homologous sequences were also identified in the 16S rRNA gene clone libraries generated for this study (data not shown).

The most striking difference between the two vent fields was the absence of known methanogens (*Methanococcaceae* and *Methanocaldococcaceae*) at Lucky Strike (Fig. 2A). This is notable because methanogens are common inhabitants of most vent fields (Takai *et al.*, 2006b), although a few single chimney surveys with limited sequencing depth have also failed to detect methanogens at other vent fields (Takai *et al.*, 2001; Hoek *et al.*, 2003; Kormas *et al.*, 2006; Zhou *et al.*, 2009). Nevertheless, this is the first report with this level of sampling and sequencing depth (12 samples, 45 195 sequences) that shows their absence at the vent field scale. The lack of detectable methanogens was confirmed by quantitative polymerase chain reaction (qPCR) assays of a functional gene diagnostic for methanogenesis (*mcrA*) in 18 vent deposits from Lucky Strike (Fig. 3). Furthermore, methanogens were not detected in 16S rRNA gene clone libraries constructed from the most diverse of the Lucky Strike samples (data not shown). The absence of methanogens at Lucky Strike in conjunction with their abundance at Rainbow is in agreement with theoretical calculations of free-energy yields for thermophilic hydrogenotrophic methanogenesis based on H_2 concentrations as previously reported (McCollom, 2007; Takai and Nakamura, 2010). Other notable differences in the archaeal communities between vent fields were observed within the *Desulfurococcaceae* at the genus level. For example, the obligate anaerobe *Staphylothermus* was prevalent in

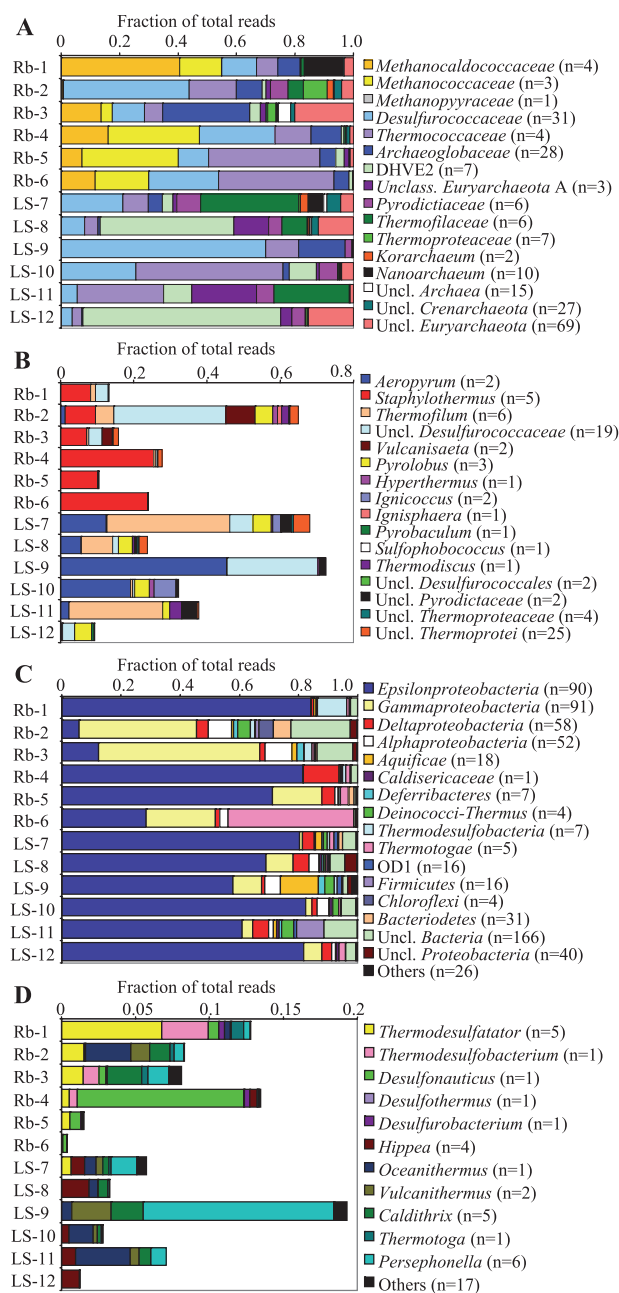


Fig. 2. Comparison of taxonomic variation in the archaeal and bacterial communities of Rainbow and Lucky Strike hydrothermal vent deposits.

A. Relative abundances of archaeal families observed in each vent deposit. Note the absence of methanogens in all Lucky Strike samples.

B. Relative abundances of crenarchaeal genera observed in each vent deposit.

C. Relative abundances of bacterial orders observed in each vent deposit.

D. Relative abundances of less abundant thermophilic genera observed in each vent deposit.

Note that the abundant, unclassified *Thermotogae* lineages shown in (C) have been omitted in (D) to allow for visualization of low-abundance genera. Numbers in parentheses following taxonomic classifications indicate the number of OTUs classified to that particular group. Rb, Rainbow; LS, Lucky Strike.

Rainbow deposits while the microaerophilic *Aeropyrum* was prevalent in Lucky Strike deposits (Fig. 2B).

SIMPER analysis (Primer v6) (Clarke and Gorley, 2006) was used to determine which archaeal genera were most responsible for the differences observed between sites (Table S3). The top four of these indicator, or 'discriminating' OTUs were two methanogens (*Methanocaldococcus* and *Methanothermococcus*) as well as *Staphylothermus* and *Aeropyrum*, which clearly points to these genera driving the differences observed between the two sites.

Models based on the geochemical characteristics of end-member fluids and their mixing styles in porous, permeable vent deposits (i.e. diffusion and advection across deposits walls bound on one side by vent fluid and the other by seawater) predict wide-oxidizing zones in exterior portions of Lucky Strike deposits and an absence of oxidizing zones in exterior portions of Rainbow deposits (Fig. 4A–C, Fig. S4A–C). The calculations were carried out as described in Tivey (2004), considering diffusion and advection of aqueous species across a porous (porosity 0.5) chimney wall bound on one side by cold seawater, and on the other by the appropriate vent fluid. Compositions of vent fluids from the Sintra and Marker 6 vents at Lucky Strike (Charlou *et al.*, 2000), and from the Flores5 vent at Rainbow (Charlou *et al.*, 2002), were used in the calculations. Concentrations of relevant aqueous species as a function of position within the chimney wall are shown in Fig. 4.

The very large differences in redox conditions for mid-to exterior layers (those at less than ~120°C) are a result of the extremes in aqueous H₂ concentrations in the different end-member fluids [16 mM at Rainbow versus 3.3 μM (Sintra) and 77 μM (Marker 6) at Lucky Strike]. Even with advection of vent fluid outward through the chimney wall, conditions of pore fluids within a chimney at the Sintra vent, Lucky Strike, would be relatively oxidizing at all temperatures up to 177°C (Fig. 4A). Other vents at Lucky Strike have higher concentrations of aqueous H₂ in end-member fluids, but conditions within a chimney at the Marker 6 vent would still be relatively oxidizing at temperatures up to 60°C (Fig. 4B). These 'relatively oxidizing zones' are zones where the free energy of the reactions for sulfide oxidation and methanotrophy are less than zero and thus favourable, while the free energy for the reactions for sulfate reduction and methanogenesis are greater than zero, and thus not favourable. Metabolic energies that would be produced from the favourable reactions at Lucky Strike (e.g. sulfide oxidation and methanotrophy) are comparable to those calculated for chimneys from other vent fields considering diffusion and advection across chimney walls (Tivey, 2004), and mixing of seawater and vent fluid (McCollom and Shock, 1997; Takai and Nakamura, 2010). Metabolic energy from methanogenesis in a Lucky Strike chimney at Marker 6

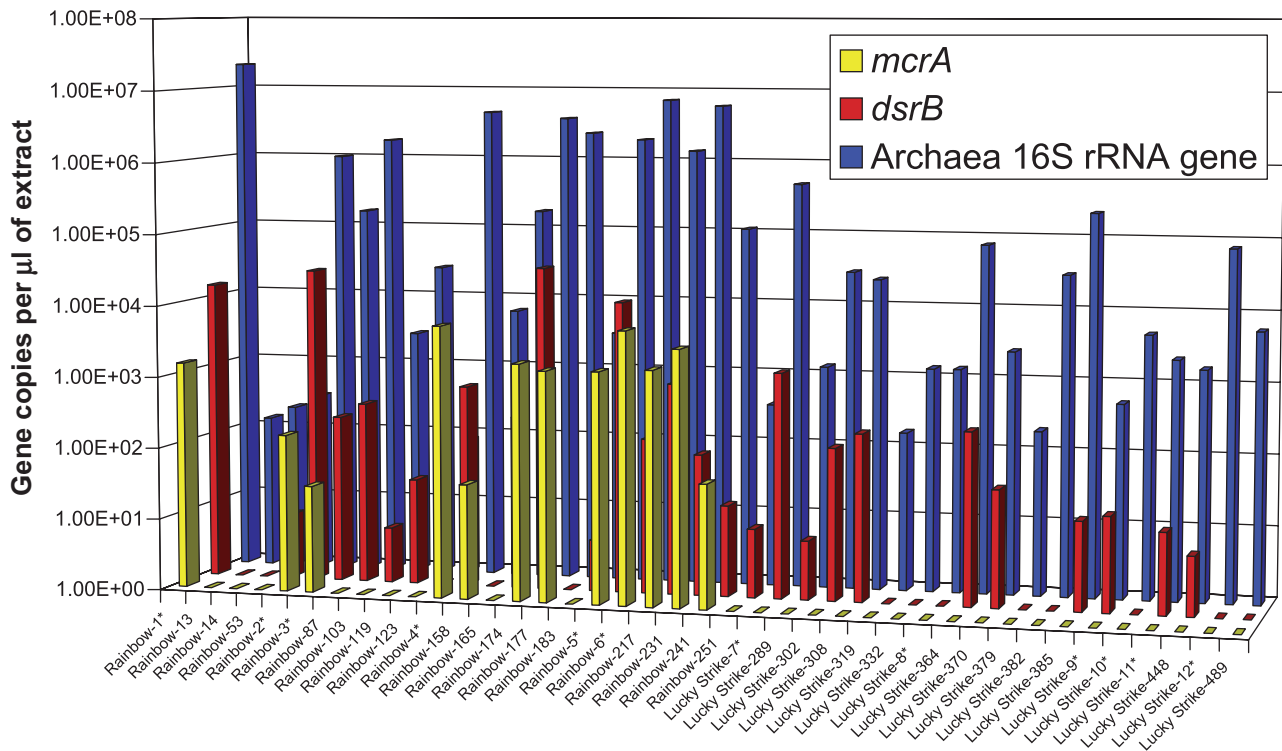


Fig. 3. Quantitative polymerase chain reaction assays targeting the gene diagnostic for methanogenesis (*mcrA*) confirms the absence of methanogens at Lucky Strike. The archaeal 16S rRNA and the dissimilatory sulfide reductase (*dsrB*) genes were also targeted in order to verify the presence of amplifiable DNA in each sample. All gene copy numbers were normalized per gram of chimney material extracted. Amplified *mcrA* and *dsrB* products were verified by cloning and sequencing of the gene (not shown). Asterisks denote samples surveyed by 454 pyrosequencing.

vent, in zones of the chimney that are at temperatures greater than 60°C, would be less than half of that from sulfate reduction.

In contrast to at Lucky Strike, the very high concentrations of aqueous H₂ in Rainbow fluids result in reducing pore fluids within all portions of Rainbow chimneys, even exterior layers surrounded by oxic seawater (Fig. 4C). Methanogenesis and sulfate reduction are energetically favourable reactions that would produce metabolic energies comparable to those calculated for reducing zones in other chimneys (Tivey, 2004) and reduced mixing zones (McCollom and Shock, 1997). On the other hand, sulfide oxidation and methanotrophy would not be expected to be favourable reactions anywhere within Rainbow chimneys, but could occur if equilibrium between H₂ and O₂ was kinetically inhibited, as proposed by Shock and Holland (2004). Laboratory experiments have demonstrated that H₂–O₂ equilibria may be kinetically inhibited at lower temperatures (Foustoukos *et al.*, 2011). The dashed lines in the bottom panels of Fig. 4 and Fig. S4 show predicted amounts of H₂ and O₂ if equilibration between the two species is completely inhibited (i.e. maximum amounts of O₂ or H₂ that might be present in zones that would be predicted to be relatively oxidizing or reducing assuming

equilibrium between the two species). For example, at the Flores5 vent at Rainbow, a very small amount of metabolic energy (an order of magnitude less than in Lucky Strike outer layers) would be available in outermost layers (e.g. at 7°C) from methanotrophy if there was complete disequilibrium between H₂ and O₂, and the amount of metabolic energy from sulfate reduction would be comparable to that in Lucky Strike exterior layers. At the low temperature of 7°C, disequilibrium might be expected (Foustoukos *et al.*, 2011). In Lucky Strike chimneys, if equilibration is completely inhibited, methanogenesis would be thermodynamically favourable in chimneys formed from Marker 6 fluids at temperatures less than 60°C, and from Sintra fluids at temperatures less than 177°C, but amounts of metabolic energy would be considerably less than from sulfide oxidation (two-thirds less for Sintra fluids, half for Marker 6 fluids). In addition, at these higher temperatures, the rate of equilibration between H₂ and O₂ would be higher than at lower temperatures (Foustoukos *et al.*, 2011).

The differences in predicted redox conditions in the exteriors of the deposits help to explain the abundance of *Aeropyrum* at Lucky Strike and *Staphylothermus* and methanogens at Rainbow. Additionally, the unusually low

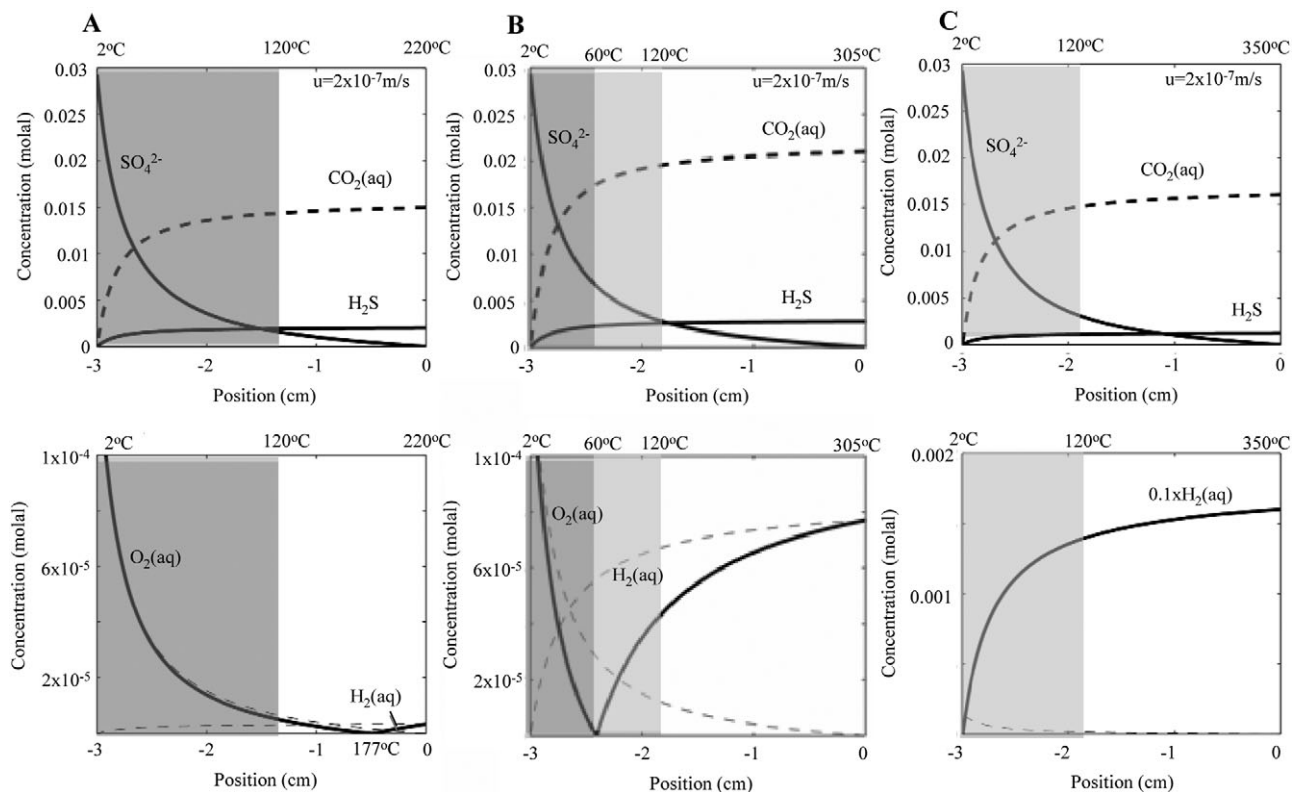


Fig. 4. Concentrations across a uniformly porous ($\phi = 0.5$) 3-cm-thick chimney wall resulting from transport between seawater (at position = -3) and (A) 220°C Sintra vent fluid (Lucky Strike), (B) 305°C Marker 6 vent fluid (Lucky Strike), (C) 350°C Flores5 vent fluid (Rainbow) at position = 0 cm by diffusion and advection of vent fluid outward at a rate of $2 \times 10^{-7} \text{ m s}^{-1}$ (u). Shading indicates where conditions at temperatures $\leq 120^\circ\text{C}$ are relatively oxidizing (dark grey) or highly reduced (light grey). Calculations were performed as described by Tivey (2004). End-member concentrations were as follows: for Flores5 $\text{H}_2 = 16 \text{ mM}$, $\text{H}_2\text{S} = 1.2 \text{ mM}$, $\text{CO}_2 = 16 \text{ mM}$; for Sintra $\text{H}_2 = 3.3 \text{ }\mu\text{M}$, $\text{H}_2\text{S} = 2 \text{ mM}$, $\text{CO}_2 = 15.1 \text{ mM}$; for Marker 6 $\text{H}_2 = 77 \text{ }\mu\text{M}$, $\text{H}_2\text{S} = 2.8 \text{ mM}$, $\text{CO}_2 = 20.7 \text{ mM}$ (from Charlou *et al.*, 2000; 2002). Note the absence of relatively oxidizing conditions within the Rainbow (Flores5) chimney versus the prediction of oxidizing conditions up to temperatures of 177°C and 60°C for Lucky Strike chimneys, depending on the concentration of aqueous H_2 in the end-member vent fluid and the advection rate. [Dashed lines in lower half of figure are for O_2 and H_2 concentrations if oxidation of H_2 is inhibited as suggested by Shock and Holland (2004)].

concentrations of H_2 in exteriors of Lucky Strike deposits (Fig. 4A–C, Fig. S4A–C) most likely cannot support methanogenesis, particularly given competition with other thermophilic hydrogen oxidizers such as members of the *Archaeoglobaceae* and *Desulfurococcaceae*. Certain members of these families would also have an advantage over methanogens by being able to use alternative electron donors when H_2 was unavailable (Boone *et al.*, 2001). Interestingly, the archaeal diversity of Rb-2 shows some similarity with those of Lucky Strike deposits (Fig. 2A). This sample is from a highly porous few-millimetre-thick distinct outer layer of a chimney (Fig. S5). The Rb-3 sample was taken from the less porous, harder interior layer adjacent to Rb-2. The fluid sampled from this vent had slightly lower measured H_2 as compared with other Rainbow fluids ($\sim 12 \text{ mmol kg}^{-1}$ versus $\sim 16 \text{ mmol kg}^{-1}$, Table S4). More efficient mixing of seawater may have occurred within the very porous (and likely more permeable) outer layer (Rb-2), which would result in

even lower H_2 , while the interior layer (Rb-3) would remain reducing and support methanogens. These findings suggest that in addition to local hydrothermal fluid chemistry influencing microbial diversity, within-field variability in archaeal diversity can be influenced by fluid mixing styles and deposit porosity and permeability.

Bacteria

Of the 91 607 bacterial V4 amplicons sequenced from the 12 hydrothermal vent samples, approximately 61% (56 091) were classified as *Epsilonproteobacteria* (Fig. 2C). *Epsilonproteobacteria* are known to play significant roles in carbon and sulfur cycling and have consistently been shown to be the most numerically abundant bacteria in these environments (Longnecker and Reysenbach, 2001; Nakagawa *et al.*, 2005b; Campbell *et al.*, 2006; Opatkiewicz *et al.*, 2009; Huber *et al.*, 2010). On a sample by sample basis, *Epsilonproteobac-*

teria were the most abundant sequences observed in three of the Rainbow and all of the Lucky Strike samples (Fig. 2C). Within the *Epsilonproteobacteria*, the moderately thermophilic *Caminibacter* and *Nautilia*, and the mesophilic *Nitratifactor* and *Sulfurovum* were detected in all samples although abundances differed likely reflecting the different temperature regimes across individual deposits (Fig. S6A). The diversity within the *Sulfurovum*, *Caminibacter* and *Nitratifactor* was surprisingly high with several OTUs identified by SIMPER as being found exclusively at one vent field (Table S5). This suggests that differences in the epsilonproteobacterial communities between Rainbow and Lucky Strike are at a finer scale (e.g. species or ecotype level) than what can be resolved with 16S rRNA gene sequences alone. These differences, however, may be significant as different OTUs within the same genus could be filling different ecological niches. For example, two hydrogen-oxidizing *Caminibacter* species previously isolated from Rainbow show differences in their oxygen tolerance as *C. mediatlanticus* is a strict anaerobe while *C. profundus* grows optimally with 0.5% oxygen (Miroshnichenko *et al.*, 2004; Voordeckers *et al.*, 2005). Therefore, although all OTUs classified as *Caminibacter* are treated equally, OTU level differences may be in response to similar geochemical properties that shape the archaeal communities. Yet, the isolated nature of these environments may also foster allopatric speciation within each vent field. Nonetheless, these results suggest that biogeographical provincialism occurs for free-living microbes as it does with vent invertebrates in deep-sea hydrothermal environments (Ramirez-Llodra *et al.*, 2007).

Of the samples not dominated by *Epsilonproteobacteria*, two were dominated by *Gammaproteobacteria* (Rb-2, -3) and one by unclassified sequences related to the *Thermotogae* (Rb-6) (Fig. 2C). Taxa of the *Gammaproteobacteria* observed in most samples include the mesophilic sulfide-oxidizing *Thiomicrospira* and several genera within the methylotrophic *Methylococcaceae* (Fig. S6B). Although two of the Rainbow deposits (Rb-1, -4) had very few sequences classified as *Gammaproteobacteria*, there was an overall greater diversity of *Methylococcaceae* at Rainbow, perhaps reflecting the higher concentrations of abiotic (and biotic) methane generated in ultramafic environments and identifying another metabolism preferentially enriched for in ultramafic environments. Because the sequences in Rb-6 are only distantly related to the *Thermotogales*, they are likely a novel deep-sea group whose primary metabolism is unknown.

Differences in the less abundant bacterial thermophilic members corroborated many of the archaeal community observations (Fig. 2D). For example, the hydrogen-oxidizing sulfate-reducing *Thermodesulfatator* and *Thermodesulfobacterium* were detected in all Rainbow

samples but were only detected in one of the Lucky Strike deposits. Within the *Deltaproteobacteria*, the genus *Desulfonauticus*, a moderately thermophilic hydrogen-oxidizing sulfate reducer, was observed in five of six Rainbow samples and not in any of the Lucky Strike deposits further suggesting enriched diversity of thermophilic hydrogen oxidizers at Rainbow. SIMPER also identified these OTUs as being some of the most significant drivers of bacterial community differences (Table S5).

Conclusions

As some studies have pointed to the possible role of subsurface geochemical processes such as phase separation as drivers for microbial diversity at vents, the small sample sizes have compromised the reported conclusions (Nakagawa *et al.*, 2005a; Nunoura and Takai, 2009). Our data from the microbial communities colonizing hydrothermal deposits show at multiple taxonomic levels that there is a direct coupling of geological, geochemical and microbiological processes at deep-sea hydrothermal vents. At the ultramafically hosted Rainbow site, the high concentrations of aqueous H₂ in the vent fluids resulting from serpentinization reactions allow for methanogens to flourish. Conversely, Lucky Strike vent fluids have very low aqueous H₂ concentrations and are oxidizing relative to most mid-ocean ridge vent fluids (Charlou *et al.*, 2000; 2002). In addition, some of the vent fluids at Lucky Strike exhibit evidence of conductive cooling in the subsurface that is attributed to the presence of impermeable cap rocks that trap fluids (Rouxel *et al.*, 2004b) and for subsurface seawater entrainment (Humphris *et al.*, 2002), which would result in venting of even more oxidizing fluids at the seafloor. Therefore, in the actively venting deposits at Lucky Strike, the conditions are not suitable for the growth of thermophilic methanogens, and favour the growth of microaerophilic hyperthermophiles.

Here we have only considered the pore fluids as the source of reduced or oxidized species that provide energy for microbial metabolism. Mineral surfaces, however, may also play a role in regulating chemical environments inhabited by microorganisms. What is known both from past studies of deposits samples at Lucky Strike and Rainbow vent fields, and from analysis of samples collected during the same cruise as this study, is that the mineral assemblages present in Rainbow versus Lucky Strike vent deposits indicate significantly more reducing conditions in Rainbow deposits, with pyrrhotite (Fe_{1-x}S) and cubanite (CuFe₂S₃) more prevalent at Rainbow and marcasite and pyrite (FeS₂) and chalcopyrite (CuFeS₂) more prevalent at Lucky Strike (Langmuir *et al.*, 1997; Rouxel *et al.*, 2004a,b). The redox state of these minerals

(more versus less reducing) may create microenvironments within the chimneys, further influencing microbial communities.

Lucky Strike and Rainbow vent fields represent opposite ends of the geochemical spectrum along the MAR hydrothermal vent fields, particularly with respect to H₂ concentrations. Extending this sampling and deep sequencing approach to other vent fields in different geologic settings and including more finer scale mineralogical and textural analyses is needed to identify the full suite of geologic and geochemical properties that influence microbial community structure and will provide boundaries for future modelling efforts.

Experimental procedures

Sample collection and DNA extraction

Vent deposit samples were collected during July/August 2008 from the Rainbow and Lucky Strike vent fields using the robotic manipulators of the remotely operated vehicle (ROV) *Jason II*. Upon collection, samples were placed in sealed, custom made bioboxes to minimize contamination from surrounding seawater. After surfacing, samples were removed from bioboxes and sampled using published methods (Reysenbach *et al.*, 2006). For samples Rainbow-1, -2, -4, -5 and Lucky Strike-7, -8, -9, -12 approximately 1–4 mm of the outer biofilm-encrusted surface was removed and homogenized using sterile mortar and pestles. For samples Lucky Strike-10 and -11, outer biofilm crusts were homogenized with inner sections as they could not be easily separated from the rock. For samples Rainbow-3 and -6, interior sections of the deposits were homogenized after removal of the outer crust. Homogenized samples were stored in cryovials at –80°C for subsequent DNA extraction. Nucleic acids for pyrosequencing, clone libraries and qPCR were extracted from homogenized samples (≈1.6–3.2 g) using the Ultra Clean Soil DNA Isolation Kit (MoBio Laboratories) according to the protocol of Reysenbach and colleagues (2006).

Hydrothermal fluid chemistry

Hydrothermal fluids were collected using isobaric gas-tight fluid samplers (Seewald *et al.*, 2002) deployed from the ROV *Jason II* and processed immediately following recovery on the ship. Vent fluid temperature was monitored continuously during fluid sampling using a thermocouple attached to the end of the sampler inlet snorkel. The reported temperatures (Table 1 and Table S4) represent maximum values recorded for each vent. Shipboard analysis of dissolved H₂ and CH₄ concentrations was accomplished using gas chromatography following headspace extraction. Samples aliquots were archived in gas-tight serum vials for shore-based determination of total dissolved CO₂ (ΣCO₂) by gas chromatography following acidification and headspace extraction. Total dissolved H₂S (ΣH₂S) and pH (25°C) were determined at sea by electrochemical

titration using a sulfide-specific electrode and a Thermo-Ross™ glass electrode, respectively.

454 Pyrosequencing

For amplifying the hypervariable V4 region of the SSU rRNA gene of *Archaea*, we used as forward primer oligonucleotides that contained a modified U519F primer sequence (Suzuki and Giovannoni, 1996) fused to 6-nucleotide key tags (Cole *et al.*, 2009) and to the 454 FLX sequencing primer A (5'-GCCTCCCTCGCGCCATCAGxxxxxx**CAGYMGCCRC GGKAAHACC**, where the x region represents the key tag and the SSU rRNA primer is bold). To allow multiplex sequencing, 10 such primers were synthesized (Integrated DNA Technologies; HPLC purified), each with a different key tag. The reverse oligonucleotide primer represented a fusion of the 454 FLX sequencing primer B and a modified Arch806R primer (Takai and Horikoshi, 2000) (5'-GCCTTGCCAGCCCGCTCAG**GGACTACNSGGTMTCTAAT**, where the 16S rRNA region is bold). PCR reactions (50 μl volume) contained 300 nM of each of forward and reverse primers, 20–50 ng of template DNA and were performed using Platinum *Taq* High Fidelity polymerase (Invitrogen, Carlsbad, CA) using the thermal profile 95°C for 2 min followed by 27 cycles of denaturation at 95°C for 15 s, primer annealing at 53°C and extension at 68°C for 45 s, with final extension of 68°C for 3 min. For a few samples the amount of template DNA was limiting and additional three to five PCR cycles were necessary in order to obtain a sufficient product. Negative control reactions without template were always performed.

The bacterial hypervariable V4 region of the SSU rRNA gene was amplified using a similar approach, using as forward primer key-tagged oligonucleotides (5'-GCCTCCCTCGCGCCATCAGxxxxxx**AYTGGGYDTAAAGNG**-3') and a mix of reverse primers (5'-GCCTTGCCAGCCCGCTCAG:**TACCRGGGTHTCTAATCC**, **:TACCAGAGTATCTAATTC**, **:CTACDSRGGTMTCTAATC** and **:TACNVGGGTA TCTAATCC**-3' in a 6:1:2:12 ratio, respectively), designed to cover most of the *Bacteria* domain (Cole *et al.*, 2009). The amplification protocol was the same as for *Archaea* except that the annealing temperature was 55°C.

The amplicon products were purified using AMPure paramagnetic beads (Agencourt Bioscience Corporation, Beverly, MA) followed by analysis of their concentration and size using DNA 1000 chips on an Agilent 2100 Bioanalyzer (Agilent Technologies, Waldbronn, Germany). Amplicon libraries were prepared for unidirectional sequencing using the emPCR Kit II (Roche) followed by sequencing on a 454 Life Sciences Genome Sequencer FLX (Roche Diagnostics, Indianapolis, IN). Based on the use of identifying key tags, 20 individual samples were pooled and sequenced on each of the two sides of the picotitre plate.

Raw sequence data were initially processed through the RDP's (Ribosomal Database Project) Pyrosequencing Pipeline (<http://pyro.cme.msu.edu/>) (Cole *et al.*, 2009). Sequences were excluded from analysis if they had a mean quality score < 20, were < 200 or > 275 bp in length (*Archaea*) (> 250 for *Bacteria*), contained ambiguous nucleotides (N's) or had any mismatches in the forward and reverse primers. The sequences were assigned to individual samples by their key tag and the 16S rRNA primers were removed prior to

analysis. Trimmed sequences were then subjected to an initial pre-classification step using the RDP classifier (Wang *et al.*, 2007) in which unclassified sequences (not *Archaea* or *Bacteria*) or sequences classified to the incorrect domain (e.g. *Bacteria* in the archaeal data set) were removed. The resulting data sets contained 207–208 nt of the bacterial and 247–249 nt of the archaeal V4 region respectively.

Sequence analysis

Trimmed sequenced files were aligned with the secondary-structure aware Infernal aligner (Nawrocki *et al.*, 2009) and clustered using the complete-linkage clustering method (furthest-neighbour) available through the RDP's pyrosequencing pipeline (Cole *et al.*, 2009). Sequences were also aligned and clustered using the SLP/PW-AL pipeline (Huse *et al.*, 2010). Individual cluster files from both methods were used to generate rarefaction curves (Colwell and Coddington, 1994) and Chao1 richness estimator (Chao and Bunge, 2002) at different OTU similarity levels (97% and 95%). Custom perl scripts were used on combined cluster files to develop abundance matrices for both archaeal and bacterial clusters. A second script was used to select representative sequences of each cluster and these sequences were run through the RDP classifier (Wang *et al.*, 2007) set at a 50% bootstrap cut-off as recommended by Claesson and colleagues (2009). Classifications were downloaded and a third script was used to link the classifications back to the original cluster files. The taxonomic results presented here were generated from the RDP OTUs at 95% similarity. We chose to use this method for analysis because the V4 region performs best with the infernal aligner used by RDP (Nawrocki *et al.*, 2009) and less stringent clustering values have been shown to minimize overestimates of diversity (White *et al.*, 2010). Selected sequences representing clusters that could not be classified by the RDP classifier were further examined by BLAST searches against the GenBank's non-redundant database (Benson *et al.*, 2009), aligning sequences in ARB (Ludwig *et al.*, 2004) and inserting them into the Silva-96 reference tree (Pruesse *et al.*, 2007) using the quick add function. When possible, clusters were then given a taxonomic classification based on published nomenclature otherwise a generic identifier (i.e. unclassified *Archaea* A) was used to track OTUs between samples.

For OTU-based beta-diversity assessments, abundance matrices were imported into Primer v6. Bray-Curtis similarities were calculated on matrices that had been normalized to total and transformed via square root while Sørensen similarities were calculated directly from abundance matrices. Distance matrices were also generated for both archaeal and bacterial communities using the phylogeny-based metric UniFrac (Lozupone *et al.*, 2006; Hamady *et al.*, 2010). First, for each of the *Bacteria* and *Archaea* global data sets we grouped the sequences in OTU clusters using either 97% or 95% sequence similarity levels, using the RDP Pyrosequencing Pipeline. We then extracted one sequence from each OTU cluster to construct hydrothermal vent reference data sets for either *Bacteria* (811 sequences at 97% and 648 sequences at 95% sequence similarity respectively) or *Archaea* (310 sequences at 97% and 229

sequences at 95% sequence similarity respectively). For tree rooting, we added the SSU rRNA sequences of either *Nanoarchaeum equitans* (GenBank AJ318041) (*Archaea* data set) or *Hydrogenobaculum* sp. (GenBank AY861719) (*Bacteria* data set), trimmed to correspond to the sequenced V4 region followed by aligning using the RDP aligner. Maximum likelihood rooted phylogenetic trees were then constructed using RAxML-7.0.4 (Stamatakis, 2006) using the GTRGAMMA parameter and 100 independent searches for the best tree. After assigning of each individual sequence from the global data sets to their closest representatives in the reference data sets using local BLAST, the UniFrac sample ID mapping file was generated using a python script, according to the Fast UniFrac data analysis flow. The online Fast UniFrac pipeline was used for the subsequent analysis, including generation of the UniFrac distance matrix. The same results were obtained using either the 97% or the 95% sequence similarity data sets. The presented figures are based on the 97% sequence similarity trees and matrices. In parallel, we also used the Greengenes core sequence data set and tree that are available as part of the online FastUniFrac for mapping and preliminary analysis, with similar results (not shown). Similarity and distance matrices were analysed using principal coordinates analysis (PCoA) (not shown), non-metric multi-dimensional scaling (NMDS), and tested for significance using ANOSIM. Additionally, similarities/distances were averaged within and between vent sites and tested for significance using a one-tailed *t*-test. All distance matrix analyses except PCoA was performed with PRIMER v6 (Clarke and Gorley, 2006).

SIMPER analysis

To help identify which organisms were responsible for the differences observed in community composition, we used SIMPER ('similarity percentages') in PRIMER v6 after classifying each OTU to the genus level (when possible) (Clarke and Gorley, 2006). The top 50 archaeal OTUs across samples were classified, imported into PRIMER v6, normalized by abundance in each sample, square-root transformed and then analysed with SIMPER. The top 100 bacterial OTUs were treated similarly with the exception that data were transformed to a presence/absence matrix to account for low abundant taxa.

Quantitative PCR (qPCR)

Quantitative PCR was performed according to manufacturer's instructions using the Quantitect SYBR green PCR kit (Qiagen, Valencia, CA) and 0.8 μ M final primer concentration, with melting curves performed at the end of each reaction to ensure product specificity. For total archaeal numbers, the protocol outlined by Reysenbach and colleagues (2006) was followed. For quantification of methanogens and sulfate reducers, qPCR with primers specific for the methyl coenzyme M reductase (*mcrA*) and the dissimilatory sulfite reductase (*dsrB*) genes was performed according to published methods (Wilson *et al.*, 2010). Gene copy numbers presented here were normalized by the amount of material in grams extracted.

Nucleotide sequence accession numbers

Nucleotide sequences generated in this study have been deposited to the NCBI Sequence Read Archive (SRP005280) (454 pyrosequencing) and in GenBank under Accession No. HQ893885-HQ894378 (clone libraries). Trimmed 454 sequences are also available at <http://alrlab.research.pdx.edu/projects/MAR2008>.

Acknowledgements

We thank the crew of the *R/V Roger Revelle* and the *DSROV Jason II* for their assistance in obtaining the samples. This research was supported by the United States National Science Foundation (OCE-0728391 and OCE-0937404 to A.-L.R.; OCE-0937392 to M.K.T.; OCE-0549829 to J.S.S.) and the US National Research Program, Water Resources Division, USGS (M.A.V. and J.D.K.). J.H.C., Z.K.Y. and M.P. were sponsored by the Laboratory Directed Research and Development Program of Oak Ridge National Laboratory (ORNL), managed by UT-Battelle, LLC for the US Department of Energy under Contract No. DE-AC05-00OR22725.

References

- Benson, D.A., Karsch-Mizrachi, I., Lipman, D.J., Ostell, J., and Sayers, E.W. (2009) GenBank. *Nucleic Acids Res* **37**: D26–D31.
- Boone, D.R., Castenholz, R.W., and Garrity, G.M. (2001) *Bergey's Manual of Systematic Bacteriology*. New York: Springer.
- Campbell, B.J., Engel, A.S., Porter, M.L., and Takai, K. (2006) The versatile *epsilon-proteobacteria*: key players in sulphidic habitats. *Nat Rev Microbiol* **4**: 458–468.
- Chao, A., and Bunge, J. (2002) Estimating the number of species in a stochastic abundance model. *Biometrics* **58**: 531–539.
- Charlou, J., Donval, J., Douville, E., Jean-Baptiste, P., Radford-Knoery, J., Fouquet, Y., *et al.* (2000) Compared geochemical signatures and the evolution of Menez Gwen (37° 50'N) and Lucky Strike (37° 17'N) hydrothermal fluids, south of the Azores Triple Junction on the Mid-Atlantic Ridge. *Chem Geol* **171**: 49–75.
- Charlou, J.L., Donval, J.P., Fouquet, Y., Jean-Baptiste, P., and Holm, N. (2002) Geochemistry of high H₂ and CH₄ vent fluids issuing from ultramafic rocks at the Rainbow hydrothermal field (36 degrees 14'N, MAR). *Chem Geol* **191**: 345–359.
- Claesson, M.J., O'Sullivan, O., Wang, Q., Nikkila, J., Marchesi, J.R., Smidt, H., *et al.* (2009) Comparative analysis of pyrosequencing and a phylogenetic microarray for exploring microbial community structures in the human distal intestine. *PLoS ONE* **4**: e6669.
- Clarke, K., and Gorley, R. (2006) PRIMER v6. User manual/tutorial Plymouth routine in multivariate ecological research Plymouth Marine Laboratory.
- Cole, J.R., Wang, Q., Cardenas, E., Fish, J., Chai, B., Farris, R.J., *et al.* (2009) The Ribosomal Database Project: improved alignments and new tools for rRNA analysis. *Nucleic Acids Res* **37**: D141–D145.
- Colwell, R.K., and Coddington, J.A. (1994) Estimating terrestrial biodiversity through extrapolation. *Philos Trans R Soc Lond B Biol Sci* **345**: 101–118.
- Desbruyeres, D., Almeida, A., Biscoito, M., Comtet, T., Khripounoff, A., Le Bris, N., *et al.* (2000) A review of the distribution of hydrothermal vent communities along the northern Mid-Atlantic Ridge: dispersal vs. environmental controls. *Hydrobiologia* **440**: 201–216.
- Desbruyeres, D., Biscoito, M., Caprais, J.C., Colaco, A., Comtet, T., Crassous, P., *et al.* (2001) Variations in deep-sea hydrothermal vent communities on the Mid-Atlantic Ridge near the Azores plateau. *Deep Sea Res Part I Oceanogr Res Pap* **48**: 1325–1346.
- Douville, E., Charlou, J.L., Oelkers, E.H., Bienvenu, P., Colon, C.F.J., Donval, J.P., *et al.* (2002) The rainbow vent fluids (36 degrees 14'N, MAR): the influence of ultramafic rocks and phase separation on trace metal content in Mid-Atlantic Ridge hydrothermal fluids. *Chem Geol* **184**: 37–48.
- Foustoukos, D., Houghton, J., Seyfried, W., Sievert, S., and Cody, G. (2011) Kinetics of H₂–O₂–H₂O redox equilibria and formation of metastable H₂O₂ under low temperature hydrothermal conditions. *Geochim Cosmochim Acta* **75**: 1594–1607.
- Hamady, M., Lozupone, C., and Knight, R. (2010) Fast UniFrac: facilitating high-throughput phylogenetic analyses of microbial communities including analysis of pyrosequencing and PhyloChip data. *ISME J* **4**: 17–27.
- Hoek, J., Banta, A., Hubler, F., and Reysenbach, A.-L. (2003) Microbial diversity of a sulphide body located in the Edmond deep-sea hydrothermal vent field on the Central Indian Ridge. *Geobiology* **1**: 119–127.
- Huber, H., Hohn, M., Rachel, R., Fuchs, T., Wimmer, V., and Stetter, K. (2002) A new phylum of Archaea represented by a nanosized hyperthermophilic symbiont. *Nature* **417**: 63–67.
- Huber, J., Mark Welch, D., Morrison, H., Huse, S., Neal, P., Butterfield, D., and Sogin, M. (2007) Microbial population structures in the deep marine biosphere. *Science* **318**: 97.
- Huber, J., Cantin, H., Huse, S., Welch, D., Sogin, M., and Butterfield, D. (2010) Isolated communities of *Epsilonproteobacteria* in hydrothermal vent fluids of the Mariana Arc seamounts. *FEMS Microbiol Ecol* **73**: 538–549.
- Humphris, S.E., Fornari, D.J., Scheirer, D.S., German, C.R., and Parson, L.M. (2002) Geotectonic setting of hydrothermal activity on the summit of Lucky Strike Seamount (37 degrees 17'N, Mid-Atlantic Ridge). *Geochem Geophys Geosyst* **3**: 1049.
- Huse, S.M., Welch, D.M., Morrison, H.G., and Sogin, M.L. (2010) Ironing out the wrinkles in the rare biosphere through improved OTU clustering. *Environ Microbiol* **12**: 1889–1898.
- Kelley, D.S., Karson, J.A., Blackman, D.K., Fruh-Green, G.L., Butterfield, D.A., Lilley, M.D., *et al.* (2001) An off-axis hydrothermal vent field near the Mid-Atlantic Ridge at 30 degrees N. *Nature* **412**: 145–149.
- Kormas, K.A., Tivey, M.K., Von Damm, K., and Teske, A. (2006) Bacterial and archaeal phylotypes associated with distinct mineralogical layers of a white smoker spire from a deep-sea hydrothermal vent site (9 degrees N, East Pacific Rise). *Environ Microbiol* **8**: 909–920.

- Langmuir, C., Humphris, S., Fornari, D., VanDover, C., VonDamm, K., Tivey, M.K., *et al.* (1997) Hydrothermal vents near a mantle hot spot: the Lucky Strike vent field at 37 degrees N on the Mid-Atlantic Ridge. *Earth Planet Sci Lett* **148**: 69–91.
- Longnecker, K., and Reysenbach, A.-L. (2001) Expansion of the geographic distribution of a novel lineage of *epsilon-Proteobacteria* to a hydrothermal vent site on the Southern East Pacific Rise. *FEMS Microbiol Ecol* **35**: 287–293.
- Lozupone, C., Hamady, M., and Knight, R. (2006) UniFrac – an online tool for comparing microbial community diversity in a phylogenetic context. *BMC Bioinformatics* **7**: 371.
- Ludwig, W., Strunk, O., Westram, R., Richter, L., Meier, H., Yadhukumar, *et al.* (2004) ARB: a software environment for sequence data. *Nucleic Acids Res* **32**: 1363–1371.
- McCollom, T.M. (2007) Geochemical constraints on sources of metabolic energy for chemolithoautotrophy in ultramafic-hosted deep-sea hydrothermal systems. *Astrobiology* **7**: 933–950.
- McCollom, T.M., and Shock, E.L. (1997) Geochemical constraints on chemolithoautotrophic metabolism by microorganisms in seafloor hydrothermal systems. *Geochim Cosmochim Acta* **61**: 4375–4391.
- Marques, A.F.A., Barriga, F., Chavagnac, V., and Fouquet, Y. (2006) Mineralogy, geochemistry, and Nd isotope composition of the Rainbow hydrothermal field, Mid-Atlantic Ridge. *Mineralium Deposita* **41**: 52–67.
- Miroshnichenko, M.L., L'Haridon, S., Schumann, P., Spring, S., Bonch-Osmolovskaya, E.A., Jeanthon, C., and Stackebrandt, E. (2004) *Caminibacter profundus* sp. nov., a novel thermophile of *Nautiliales* ord. nov. within the class '*Epsilonproteobacteria*', isolated from a deep-sea hydrothermal vent. *Int J Syst Evol Microbiol* **54**: 41–45.
- Moussard, H., Moreira, D., Cambon-Bonavita, M., López-García, P., and Jeanthon, C. (2006) Uncultured Archaea in a hydrothermal microbial assemblage: phylogenetic diversity and characterization of a genome fragment from a euryarchaeote. *FEMS Microbiol Ecol* **57**: 452–469.
- Nakagawa, S., Takai, K., Inagaki, F., Chiba, H., Ishibashi, J., Kataoka, S., *et al.* (2005a) Variability in microbial community and venting chemistry in a sediment-hosted backarc hydrothermal system: impacts of seafloor phase-separation. *FEMS Microbiol Ecol* **54**: 141–155.
- Nakagawa, S., Takai, K., Inagaki, F., Hirayama, H., Nunoura, T., Horikoshi, K., and Sako, Y. (2005b) Distribution, phylogenetic diversity and physiological characteristics of *epsilon-Proteobacteria* in a deep-sea hydrothermal field. *Environ Microbiol* **7**: 1619–1632.
- Nawrocki, E.P., Kolbe, D.L., and Eddy, S.R. (2009) Infernal 1.0: inference of RNA alignments. *Bioinformatics* **25**: 1335–1337.
- Nunoura, T., and Takai, K. (2009) Comparison of microbial communities associated with phase-separation-induced hydrothermal fluids at the Yonaguni Knoll IV hydrothermal field, the Southern Okinawa Trough. *FEMS Microbiol Ecol* **67**: 351–370.
- Opatkiewicz, A.D., Butterfield, D.A., and Baross, J.A. (2009) Individual hydrothermal vents at Axial Seamount harbor distinct seafloor microbial communities. *FEMS Microbiol Ecol* **70**: 413–424.
- Page, A., Tivey, M.K., Stakes, D.S., and Reysenbach, A.-L. (2008) Temporal and spatial archaeal colonization of hydrothermal vent deposits. *Environ Microbiol* **10**: 874–884.
- Perner, M., Kuever, J., Seifert, R., Pape, T., Koschinsky, A., Schmidt, K., *et al.* (2007) The influence of ultramafic rocks on microbial communities at the Logatchev hydrothermal field, located 15 degrees N on the Mid-Atlantic Ridge. *FEMS Microbiol Ecol* **61**: 97–109.
- Pruesse, E., Quast, C., Knittel, K., Fuchs, B.M., Ludwig, W., Peplies, J., and Glockner, F.O. (2007) SILVA: a comprehensive online resource for quality checked and aligned ribosomal RNA sequence data compatible with ARB. *Nucleic Acids Res* **35**: 7188–7196.
- Ramirez-Llodra, E., Shank, T.M., and German, C.R. (2007) Biodiversity and biogeography of hydrothermal vent species. *Oceanography* **20**: 30–41.
- Reysenbach, A.-L., and Flores, G.E. (2008) Electron microscopy encounters with unusual thermophiles helps direct genomic analysis of *Aciduliprofundum boonei*. *Geobiology* **6**: 331–336.
- Reysenbach, A.-L., Liu, Y., Banta, A.B., Beveridge, T.J., Kirshstein, J.D., Schouten, S., *et al.* (2006) A ubiquitous thermoacidophilic archaeon from deep-sea hydrothermal vents. *Nature* **442**: 444–447.
- Rouxel, O., Fouquet, Y., and Ludden, J.N. (2004a) Copper isotope systematics of the Lucky Strike, Rainbow, and Logatchev sea-floor hydrothermal fields on the Mid-Atlantic Ridge. *Econ Geol* **99**: 585–600.
- Rouxel, O., Fouquet, Y., and Ludden, J.N. (2004b) Subsurface processes at the Lucky Strike hydrothermal field, Mid-Atlantic Ridge: evidence from sulfur, selenium, and iron isotopes. *Geochim Cosmochim Acta* **68**: 2295–2311.
- Sarrazin, J., and Juniper, S.K. (1999) Biological characteristics of a hydrothermal edifice mosaic community. *Mar Ecol Prog Ser* **185**: 1–19.
- Schloss, P. (2010) The effects of alignment quality, distance calculation method, sequence filtering, and region on the analysis of 16S rRNA gene-based studies. *PLoS Comput Biol* **6**: e1000844.
- Schmidt, K., Koschinsky, A., Garbe-Schonberg, D., de Carvalho, L.M., and Seifert, R. (2007) Geochemistry of hydrothermal fluids from the ultramafic-hosted Logatchev hydrothermal field, 15 degrees N on the Mid-Atlantic Ridge: temporal and spatial investigation. *Chem Geol* **242**: 1–21.
- Seewald, J.S., Doherty, K.W., Hammar, T.R., and Liberatore, S.P. (2002) A new gas-tight isobaric sampler for hydrothermal fluids. *Deep Sea Res Part I Oceanogr Res Pap* **49**: 189–196.
- Seyfried, W.E., Pester, N.J., Ding, K., and Rough, M. (2011) Vent fluid chemistry of the Rainbow Hydrothermal System (36°N, MAR): phase equilibria and *in-situ* pH controls on seafloor alteration processes. *Geochim Cosmochim Acta* **75**: 1574–1593.
- Shock, E.L., and Holland, M.E. (2004) Geochemical energy sources that support the subsurface biosphere. In *Subseafloor Biosphere at Mid-ocean Ridges*. Wilcock, W., Cary, C., DeLong, E., Kelley, D., and Baross, J. (eds). Washington, DC, USA: American Geophysical Union, pp. 153–165.
- Shock, E.L., McCollom, T., and Schulte, M.D. (1995)

- Geochemical constraints on chemolithoautotrophic reactions in hydrothermal systems. *Orig Life Evol Biosph* **25**: 141–159.
- Singh, S.C., Crawford, W.C., Carton, H., Seher, T., Combiér, V., Cannat, M., *et al.* (2006) Discovery of a magma chamber and faults beneath a Mid-Atlantic Ridge hydrothermal field. *Nature* **442**: 1029–1032.
- Sogin, M.L., Morrison, H.G., Huber, J.A., Mark Welch, D., Huse, S.M., Neal, P.R., *et al.* (2006) Microbial diversity in the deep sea and the underexplored 'rare biosphere'. *Proc Natl Acad Sci USA* **103**: 12115–12120.
- Stamatakis, A. (2006) RAxML-VI-HPC: maximum likelihood-based phylogenetic analyses with thousands of taxa and mixed models. *Bioinformatics* **22**: 2688–2690.
- Suzuki, M.T., and Giovannoni, S.J. (1996) Bias caused by template annealing in the amplification of mixtures of 16S rRNA genes by PCR. *Appl Environ Microbiol* **62**: 625–630.
- Takai, K., and Horikoshi, K. (1999) Genetic diversity of archaea in deep-sea hydrothermal vent environments. *Genetics* **152**: 1285–1297.
- Takai, K., and Horikoshi, K. (2000) Rapid detection and quantification of members of the archaeal community by quantitative PCR using fluorogenic probes. *Appl Environ Microbiol* **66**: 5066–5072.
- Takai, K., and Nakamura, K. (2010) Compositional, physiological and metabolic variability in microbial communities associated with geochemically diverse, deep-sea hydrothermal vent fluids. In *Geomicrobiology: Molecular and Environmental Perspective*. Barton, L.L., Mandl, M., and Loy, A. (eds). New York, NY, USA: Springer, pp. 251–283.
- Takai, K., Komatsu, T., Inagaki, F., and Horikoshi, K. (2001) Distribution of archaea in a black smoker chimney structure. *Appl Environ Microbiol* **67**: 3618–3629.
- Takai, K., Gamo, T., Tsunogai, U., Nakayama, N., Hirayama, H., Nealson, K.H., and Horikoshi, K. (2004) Geochemical and microbiological evidence for a hydrogen-based, hyperthermophilic subsurface lithoautotrophic microbial ecosystem (HyperSLiME) beneath an active deep-sea hydrothermal field. *Extremophiles* **8**: 269–282.
- Takai, K., Nakamura, K., Suzuki, K., Inagaki, F., Nealson, K., and Kumagai, H. (2006a) Ultramafics–Hydrothermalism–Hydrogenesis–HyperSLiME (UltraH3) linkage: a key insight into early microbial ecosystem in the Archean deep-sea hydrothermal systems. *Paleontol Res* **10**: 269–282.
- Takai, K., Nakagawa, T., Reysenbach, A.-L., and Hoek, J. (2006b) Microbial ecology of Mid-Ocean Ridges and Back-Arc Basins. In *Back-Arc Spreading Systems: Geological, Biological, Chemical, and Physical Interactions*. Christie, D.M., Fisher, C.R., Sang-Mook, L., and Givens, S. (eds). Washington, DC, USA: American Geophysical Union, pp. 185–213.
- Takai, K., Nunoura, T., Ishibashi, J., Lupton, J., Suzuki, R., Hamasaki, H., *et al.* (2008) Variability in the microbial communities and hydrothermal fluid chemistry at the newly discovered Mariner hydrothermal field, southern Lau Basin. *J Geophys Res* **113**: G02031.
- Tivey, M.K. (2004) Environmental conditions within active seafloor vent structures: sensitivity to vent fluid composition and fluid flow. In *Subseafloor Biosphere at Mid-Ocean Ridges*. Wilcock, W., Cary, C., DeLong, E., Kelley, D., and Baross, J. (eds). Washington, DC, USA: American Geophysical Union, pp. 137–152.
- Tivey, M.K. (2007) Generation of seafloor hydrothermal vent fluids and associated mineral deposits. *Oceanography* **20**: 50–65.
- Von Damm, K.L. (1995) Controls on the chemistry and temporal variability of seafloor hydrothermal fluids. In *Seafloor Hydrothermal Systems: Physical, Chemical, Biological, and Geological Interactions*. Humphris, S.E., Zierenberg, R.A., Mullineaux, L.S., and Thomson, R.E. (eds). Washington, DC, USA: American Geophysical Union, pp. 222–247.
- Von Damm, K., Bray, A., Buttermore, L., and Oosting, S. (1998) The geochemical controls on vent fluids from the Lucky Strike vent field, Mid-Atlantic Ridge. *Earth Planet Sci Lett* **160**: 521–536.
- Voordeckers, J.W., Starovoytov, V., and Vetriani, C. (2005) *Caminibacter mediatlanticus* sp. nov., a thermophilic, chemolithoautotrophic, nitrate-ammonifying bacterium isolated from a deep-sea hydrothermal vent on the Mid-Atlantic Ridge. *Int J Syst Evol Microbiol* **55**: 773–779.
- Wang, Q., Garrity, G.M., Tiedje, J.M., and Cole, J.R. (2007) Naive Bayesian classifier for rapid assignment of rRNA sequences into the new bacterial taxonomy. *Appl Environ Microbiol* **73**: 5261–5267.
- White, J.R., Navlakha, S., Nagarajan, N., Ghodsi, M.R., Kingsford, C., and Pop, M. (2010) Alignment and clustering of phylogenetic markers – implications for microbial diversity studies. *BMC Bioinformatics* **11**: 152.
- Wilson, T., Amirbahman, A., Norton, S., and Voytek, M. (2010) A record of phosphorus dynamics in oligotrophic lake sediment. *J Paleolimnol* **44**: 279–294.
- Zhou, H., Li, J., Peng, X., Meng, J., Wang, F., and Ai, Y. (2009) Microbial diversity of a sulfide black smoker in main endeavour hydrothermal vent field, Juan de Fuca Ridge. *J Microbiol* **47**: 235–247.

Supporting information

Additional Supporting Information may be found in the online version of this article:

Fig. S1. Photographs of hydrothermal vent samples collected from the Rainbow and Lucky Strike vent fields. Yellow circles indicate which chimney/section was used for sampling.

Fig. S2. Rarefaction analysis illustrates the greater diversity observed in the bacterial communities of 12 hydrothermal deposit samples collected from the Rainbow and Lucky Strike vent fields.

A. Archaeal rarefaction curves at two sequence similarity levels (97% and 95%) using two different alignment/clustering methods. Note the near-asymptotic appearance of several curves suggesting nearly complete sampling of the V4 sequences.

B. Bacterial rarefaction curves.

Rb, Rainbow; LS, Lucky Strike.

Fig. S3. 16S rRNA gene surveys reveal partitioning of the archaeal and bacterial communities between the ultramafic

hosted Rainbow (red) and basalt-hosted Lucky Strike (blue) vent fields along the Mid-Atlantic Ridge. Communities clustered using MDS of the unweighted (A and D) and weighted (B and E) UniFrac distances for archaeal (A, B) and bacterial (D, E) communities. Sorensen similarity values for archaeal (C) and bacterial (F) communities also clustered by vent site. Each point represents an individual vent sample. Results of ANOSIM analysis showing that the observed patterns are significant are presented in the bottom right or left corner of each plot. (G) Average unweighted and weighted (H) UniFrac distance within and between vent fields. Average distances were significantly different for archaeal weighted ($P < 0.01$) and unweighted ($P < 0.001$), and bacterial unweighted ($P < 0.001$) communities as determined by one-tailed t -tests. Sorensen similarities were also significantly different (I) for both bacteria ($P < 0.001$) and archaea ($P < 0.001$). Error bars indicate the standard error of the mean (SEM).

Fig. S4. Concentrations across a uniformly porous ($\phi = 0.5$) 3-cm-thick chimney wall resulting from transport between seawater (at position = -3) and (A) 220°C Sintra vent fluid (Lucky Strike), (B) 305°C Marker 6 vent fluid (Lucky Strike), (C) 350°C Flores5 vent fluid (Rainbow) at position = 0 by diffusion only (see Fig. 4 caption for more details of calculations). Note the lack of oxidizing zone for the Rainbow chimney even with no outward advection of vent fluid.

Fig. S5. Photograph of the hydrothermal vent chimney used for samples Rb-2 and Rb-3. Note how the porous, outer layer (Rb-2) cleanly peels away from the rest of the chimney sample.

Fig. S6. Comparison of taxonomic variation in the bacterial communities of Rainbow and Lucky Strike hydrothermal vent deposits.

A. Relative abundances of epsilonproteobacterial genera observed in each vent deposit.

B. Relative abundances of gammaproteobacterial families observed in each vent deposit.

Numbers in parentheses following taxonomic classifications indicate the number of OTUs classified to that particular group. Rb, Rainbow; LS, Lucky Strike.

Table S1. Hydrothermal vent deposits used to characterize the microbial communities from the Rainbow (Rb) and Lucky Strike (LS) vent fields.

Table S2. Comparison of OTU richness and Chao1 diversity estimates generated from two different clustering methods for archaeal and bacterial communities of hydrothermal vent deposits collected along the Mid-Atlantic Ridge.

Table S3. SIMPER analysis was used to identify archaeal genera responsible for the dissimilarity observed in the communities of Rainbow and Lucky Strike vent deposits.

Table S4. End-member fluid chemistry of samples used for microbial community characterizations.

Table S5. SIMPER analysis was used to identify bacterial genera responsible for the dissimilarity observed in the communities of Rainbow and Lucky Strike vent deposits.

Please note: Wiley-Blackwell are not responsible for the content or functionality of any supporting materials supplied by the authors. Any queries (other than missing material) should be directed to the corresponding author for the article.